Z. Kristallogr. Suppl. **26** (2007) 223-228

X-ray diffraction analysis of an ε/γ′ iron-nitride compound double layer

T. Gressmann[1], A. Leineweber[1,*], E.J. Mittemeijer[1], M. Knapp[2]

[1]Max Planck Institute for Metals Research, Heisenbergstraße 3, D-70569 Stuttgart, Germany
[2]Institute for Materials Science, Darmstadt University of Technology, Petersenstr. 23, D-64287 Darmstadt, Germany; Present address: CELLS, P.O.B. 68, E-08193 Barcelona, Spain
[*] Contact author; e-mail: a.leineweber@mf.mpg.de

Keywords: iron nitrides, stress determination, diffraction-line broadening, elastic anisotropy

Abstract. An ε-Fe_3N/γ′-Fe_4N double compound layer grown on α-Fe was investigated by X-ray diffraction analysis. The anisotropic diffraction-line broadening observed by high-resolution synchrotron diffraction measurements and the diffraction-line shifts as measured for hexagonal ε layer can be quantitatively explained by the presence of both a lattice parameter gradient associated with a concentration gradient and a stress gradient within the layer. Investigation of the γ′ layer revealed an elastic anisotropy unusual for *fcc* type metals.

Introduction

Treatment of ferritic iron and steel by nitriding at temperatures between 773 K and 853 K in NH_3/H_2 gas mixtures usually leads to the formation of iron-nitride layers at the workpiece surfaces, which improve the wear and corrosion resistance [1]. Such compound layers on pure iron are, if sufficient N is provided by the atmosphere, composed of an outer ε-Fe_3N_{1+x} sublayer adjacent to the surface and an inner γ′-Fe_4N sublayer adjacent to the layer/substrate interface (figure 1). Both, the ε and the γ′ phase contain closed-packed stacking of iron atoms (ε: *hcp*; γ′: *fcc*) in which the N atoms occupy octahedral interstitial sites in a long-range ordered fashion [2, 3].

The homogeneity range of ε-Fe_3N_{1+x} extends from about 24 to 33 at.% N at 823 K [4] associated with considerable variation of the lattice parameters *a* and *c* [5, 6]. Due to the inward diffusion of N during the nitriding process a concentration-depth profile builds up within the ε layer with high N content at the surface and low N content at the ε/γ′ interface causing a depth dependence of the lattice parameters *a* and *c*. Furthermore, a macrostress-depth profile will likely build up within the layer (i) during growth due to the nitrogen concentration-depth profile, which contributes to the depth dependence of the lattice parameters *a* and *c* and (ii) after

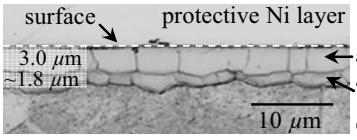

Figure 1: Cross-sectional optical micrograph of the nitrided (1.5 h, 823 K, 56/44 vol.% NH_3/H_2) α-Fe specimen with an ε/γ′ compound double layer

growth during cooling due to different coefficients of thermal expansion of the layer and the substrate [7]. γ′-Fe_4N on the other hand is largely stoichiometric (20 at.% N); its residual stresses are mainly thermally induced, but also effects due to the slight concentration gradient come into play [8].
The present paper deals with different aspects of ε/γ′ iron-nitride compound double layers investigated by X-ray diffraction including high-resolution diffraction experiments using synchrotron radiation. The first part deals with diffraction-line broadening and shifts due to both concentration- and stress-depth profiles of ε-Fe_3N_{1+x}, whereas in the second part X-ray stress measurements of the γ′-Fe_4N layer are analysed.

Experimental

A cold-rolled and recrystallised pure iron plate of about 1 mm thickness was nitrided at 823 K in a vertical quartz-tube furnace (diameter 28 mm) for 1.5 h in a nitriding atmosphere composed of 56 vol.% NH_3 and 44 vol.% H_2 (flow rate 500 ml/min). After nitriding the sample was quenched by dropping it into water. The compound-layer thickness was determined on cross sections by means of optical microscopy as described elsewhere [9, 10] (figure 1).
X-ray powder diffraction measurements of the nitrided specimen were performed:

- at the high-resolution beamline B2 [11] (HASYLAB, Hamburg) for the ε phase (110, 002, 111, 112, 300, 113, 302, 223, 304 reflections) and for selected γ′ reflections (111, 220, 311, 420) employing synchrotron radiation (λ = 0.80017 Å). Additionally, SRM660a LaB_6 (NIST, USA) and an under vacuum annealed ε layer (1 day at 673 K) in order to remove the concentration gradient [10] were measured.
- *in house* on a PANalytical MRD instrument (CoKα radiation: $\lambda_{\alpha 1}$ = 1.78897 Å, $\lambda_{\alpha 2}$ = 1.79285 Å; quasi-parallel beam, divergence ~0.3°; secondary graphite monochromator) for γ′ reflections which do not show peak-overlap with ε reflections.

Both instruments were equipped with a Eulerian cradle and during all measurements the sample was rotated around the surface normal in order to achieve better crystallite statistics (a rotationally symmetric state of stress was assumed). Both diffractometers were used in χ mode[1] [12] in symmetrical diffraction geometry (ψ tilt ranged between 0° and 60°: step width varied between 7.5° and 30° depending on the diffractometer and the reflection).

Concentration- and stress-depth profiles in the ε-Fe_3N_{1+x} layer

Model for the microstructure of the ε layer
A depth(z)-dependent N content in the ε layer (thickness Z) implies depth-dependent hexagonal lattice parameters $a(z)$ and $c(z)$; for each *hkl* the depth-dependent (stress-free) lattice spacing $d_{hkl,0}(z)$ can be calculated. The additional presence of depth-dependent macrostress $\sigma_{//}(z)$ parallel to the surface will lead to a ψ-dependent modification of the d-spacing of a reflection *hkl*: $d_{hkl,\psi}(z) \neq d_{hkl,0}(z)$ (see what follows).
For practical purposes it was assumed that $a(z)$ and $c(z)$ vary independently linearly between each pair of equidistant adjacent grid points. The grid points are located at depths $z_j = jZ/5$

[1] χ is the angle of rotation of the sample around the axis defined by the intersection of the diffraction plane and the sample surface, i.e. perpendicular to the $\theta/2\theta$ plane; χ coincides in χ mode with the angle ψ.

(j = 0,1...5), at which the lattice parameters are a_j and c_j. This leads to a similar partitioning of $d_{hkl,0}(z)$ with z (cf. figure 2). Furthermore, it is assumed that a linear stress-depth profile occurs. Then, the d-spacing of a set of lattice planes (hkl) with a normal vector tilted by an angle ψ with respect to the specimen surface normal can be calculated according to

$$\left(d_{hkl,\psi}(z) - d_{hkl,0}(z)\right) / d_{hkl,0}(z) = \left(2S_1^{hkl} + \tfrac{1}{2} S_2^{hkl} \cdot \sin^2 \psi\right) \sigma_{//}(z) \qquad (1)$$

where S_1^{hkl} and $\frac{1}{2}S_2^{hkl}$ are the X-ray elastic constants (XECs) calculated from single-crystal elastic constants (SECs) calculated for ε-Fe_3N by first-principles methods [13] adopting the Neerfeld-Hill model for grain interaction and neglecting the effect of the presence of a moderate texture in the ε layer. Note that this treatment neglects the fact that for a given reflection hkl and at a given tilt angle ψ differently oriented (with respect to the planar macrostress) crystallites, which are likely slightly differently strained, may lead to an additional line broadening contribution.

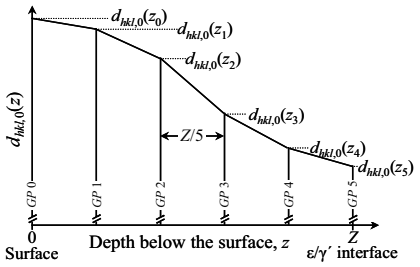

Figure 2: Schematic presentation of the sectioning of the ε layer using equidistant grid points (GP) with the corresponding strain-free lattice spacings $d_{hkl,0}(z_j)$.

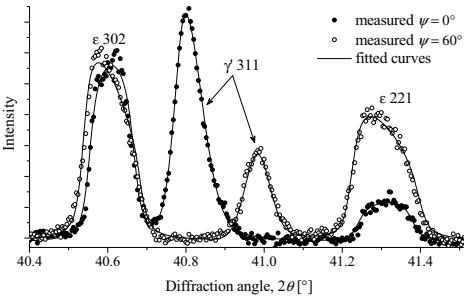

Figure 3: Part of the diffraction patterns recorded at ψ = 0° and ψ = 60° of the ε/γ′ compound layer and the obtained fitted curves.

On the basis of the above model the diffraction profiles of the ε layer in principle can be calculated. It will be assumed that coherency effects between regions of different lattice spacings can be neglected. Then, for a given hkl, the reflection profile on the diffraction angle scale is obtained by summing up the intensities arising from sublayers at z = 0 to $z = Z$ with their corresponding d-spacing $d_{hkl,\psi}(z)$, taking into account for each depth z the effect of X-ray attenuation as described by multiplying the intensity with $\exp(-\mu(\lambda)k_{hkl,\psi}z)$, where $\mu(\lambda)$ is the (effective) linear absorption coefficient of the probed material at the applied wavelength λ, $k_{hkl,\psi}$ is a diffraction-geometry dependent factor [14], which reads in the present case $k_{hkl,\psi} = 2/(\sin\theta_{hkl} \cos\psi)$.

Diffraction-line profile fitting was performed for all recorded reflections *simultaneously* (at all tilt angles ψ) using the program Topas [15] by treating the ε phase as a single "hkl phase" ("Pawley fits") with an anisotropic line broadening and shifting contribution due to lattice parameter variations [16], stress effects and absorption as described above. The independently fitted stress-free lattice parameters a_j and c_j at the grid points were treated during the refinement with a penalty function "punishing" the deviation of the whole $a(z)$ and $c(z)$ profiles from a completely linear one [13]. The stress profile has only the fit parameters: value of the stress at the sample's surface and the (constant) stress gradient. The described physical broadening contributions were convoluted with a fixed instrumental broadening function

determined on the basis of LaB_6 standard measurements and a fixed physical broadening contribution measured from a homogenised ε-Fe_3N_{1+x} layer during refinement [13].

Results and discussion

The observed ε reflections exhibit a considerable, anisotropic line broadening, in particular for reflections with diffraction vectors close to the a^*b^* plane, i.e. those with large $|h|$ and $|k|$ and small $|l|$ (figure 3), as expected due to the anisotropy of the lattice-parameter changes due to compositional variation [16]. By fitting - using the described model in the previous section - the observed profiles can be reproduced well; slight problems only occur for the peak positions of reflections with diffraction vectors close to **c***, e.g. 00*l*, 113. These problems may be associated with an inability of the XECs obtained from the calculated SEC to describe all stress-induced peak shifts (cf. equation 1) appropriately.

The obtained depth-dependent strain-free lattice parameters (figure 4) appear only partially compatible with the variation of the N content expected from the nitriding conditions, i.e. from 25.7 at.% N at the surface [17] to 24.1 at.% N at the ε/γ′ interface [4] and previously reported composition-dependencies for *a* and *c* [5, 6]. Best agreement is found for *a* and *c* values measured at the surface and for those reported in Ref. [5]. With increasing distance to the surface the fitted stress-free lattice parameters systematically deviate from the dependence of *c* vs. *a* as expected from [5, 6]: The observed *c* values vary much less than as expected from the simultaneously observed variation of *a* (figure 4).

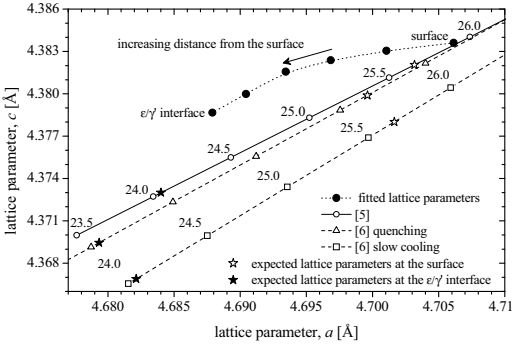

Figure 4: Lattice parameter c vs. lattice parameter a plot for the fitted depth profile (full points) within the ε layer together with corresponding relations from [5, 6]. The open points represent calculated N contents in at.% and the stars the from the nitriding conditions expected lattice parameters at the surface and at the ε/γ′ interface.

The deviations of the observed behaviour of *c* vs. *a* from those given by [5, 6] may be caused by microstructural aspects, e.g. stress fields in the (columnar) crystallites due to the concentration gradients, which are not accounted for in the modelling. Furthermore, the stresses in the ε layer may influence the state of N ordering in the ε-phase superstructure and the magnetism, which can influence the lattice parameters measured on powders [6].

Simultaneous analysis of the residual macrostresses revealed tensile stresses of about 90 MPa at the surface, and the presence of a stress gradient leading to compressive stresses of about –95 MPa at the ε/γ′ interface, which is also in agreement with some basic trends observed by Somers [7] and references therein. This state of stress can be understood (assuming the absence of layer-growth stresses at the nitriding temperature) as thermally induced by quenching after nitriding due to different linear expansion coefficients of the ε layer and the α-Fe substrate. The stress gradient can be explained mainly by a N-concentration dependence of the coefficient of thermal expansion of the ε phase [18] (the thermal expansion coefficients of α-Fe falls within the range of coefficients possible for the ε phase), which is larger for high

N content as prevailing at the surface and smaller for low N content as prevailing at the ε/γ′ interface. The stress gradient also leads effectively to an additional ψ-dependent diffraction line broadening (cf. figure 3).

Stresses in the γ′-Fe_4N layer

Residual stress-depth profiles in γ′ monolayers have been investigated in detail previously [8] and the observed stresses could be understood as both thermally induced and compositionally induced. So far only one single reflection (mostly γ′ 420) has been used for stress determination in γ′ layers, therefore, effects arising from elastic anisotropy of γ′ have not been considered. However, ab-initio calculations predict that γ′-Fe_4N is elastically anisotropic [9], where the anisotropy is reverse to that of usual *fcc*-type metals, i.e. in γ′-Fe_4N the <111> directions instead of the <100> directions are the most compliant ones.

Indeed, the slopes $\left|\tfrac{1}{2}S_2^{hkl}\sigma_{//}\right|$ in ε_{hkl} vs. $\sin^2\psi$ plots as observed in this study are orientation dependent. $\left|\tfrac{1}{2}S_2^{hkl}\sigma_{//}\right|$ is smaller in <*h*00> than in <*hhh*> direction (figure 5), confirming the theoretically predicted anisotropy [9].

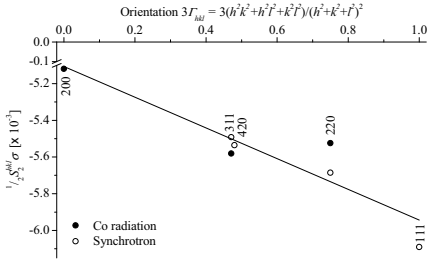

Figure 5: hkl dependence of the slopes $^1/_2S_2\sigma_{//}$ of ε_{hkl} vs. $\sin^2\psi$ plots demonstrating the elastic anisotropy of γ′-Fe_4N

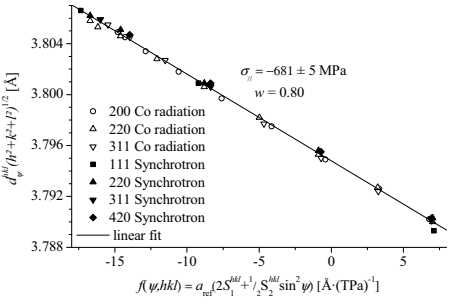

Figure 6: Stress analysis employing the f(ψ) method

Quantitative stress analysis was performed by means of the $f(\psi)$ method [12], simultaneously using a series of different *hkl* reflections measured at different tilt angles ψ. In this method $d_\psi^{hkl}(h^2+k^2+l^2)^{1/2}$ is plotted versus $f(\psi) = a_{ref}\,(2S_1^{hkl} + \tfrac{1}{2}S_2^{hkl}\sin^2\psi)$, yielding a straight line with the slope corresponding to $\sigma_{//}$. a_{ref} is a reference lattice parameter with a value close to the strain-free lattice parameter. The $f(\psi)$ method was also used to determine simultaneously effective X-ray elastic constants according to

$$S_{1,2}^{hkl} = wS_{1,2}^{V} + (1-w)S_{1,2}^{R} \qquad (2)$$

during stress determination by least-squares fitting to the data (figure 6) with $\sigma_{//}$ and w as fit parameters, where w is a weighting parameter between the Voigt (V) and Reuss (R) type grain interaction [19]. The determined compressive stress of –681 ± 5 MPa (averaged over the layer thickness) is in good agreement with stress values found in literature [8]. The fitted value of the weighting parameter $w = 0.8$ revealed a distinct Voigt-like type of grain interaction. There are various possible explanations for this type of grain interaction, which will be discussed in detail in reference [9].

Conclusions

By X-ray diffraction different microstructural aspects of ε/γ′ iron-nitride compound surface double layers have been investigated. A model was proposed with which one can describe both anisotropic line broadening and macrostress-originated shifting of diffraction lines. The model was successfully applied to high-resolution synchrotron measurements on a hexagonal ε-Fe_3N_{1+x} layer. The peak broadening was mainly due to an N concentration-depth profile within the ε layer, whereas the peak shifts are caused by a stress-depth profile originating from the concentration-dependence of the coefficient of thermal expansion of the ε phase.
X-ray stress measurements on the γ′-Fe_4N layer using several different *hkl*-reflections revealed an unusual anisotropy for *fcc*-type metals: <100> as the stiffest direction and <111> as the most compliant direction. Stress determination was performed on the basis of the $f(\psi)$ method confirming the presence of compressive stress much larger than within the ε layer, and revealing a mostly Voigt-like type of grain interaction.

References

1. Liedtke, D., Baudis, U., Boßlet, J., Huchel, U., Klümper-Westkamp, H., Lerche, W. Spies, H.-J., 2006, *Wärmebehandlung von Eisenwerkstoffen* (Renningen: Expert Verlag).
2. Jack, K.H., 1948, *Proc. R. Soc. London, A*, **195**, 34.
3. Jack, K.H., 1952, *Acta Crystallogr*, **5**, 404.
4. Wriedt, H.A., Gokcen, N.A. & Nafziger, R.H., 1987, *Bull Alloy Phase Diagr*, **8**, 355.
5. Somers, M.A.J., Kooi, B.J., Maldzinski, L., Mittemeijer, E.J., van der Horst, A.A., van der Kraan, A.M. & van der Pers, N.M., 1997, *Acta Mater.*, **45**, 2013.
6. Liapina, T., Leineweber, A., Mittemeijer, E.J. & Kockelmann, W., 2004, *Acta Mater.*, **52**, 173.
7. Somers, M.A.J. & Mittemeijer, E.J., 1992, *Härterei-Tech. Mitt.*, **47**, 175.
8. Somers, M.A.J. & Mittemeijer, E.J., 1990, *Metall. Trans. A*, **21A**, 189.
9. Gressmann, T., Wohlschlögel, M., Shang, S., Welzel, U., Leineweber, A., Mittemeijer, E.J. & Liu, Z.-K., *in preparation*.
10. Liapina, T., Leineweber, A. & Mittemeijer, E.J., 2006, *Metall. Mater. Trans. A*, **37A**, 319.
11. Knapp, M., Baehtz, C., Ehrenberg, H. & Fuess, H., 2004, *J. Synchr. Rad.*, **11**, 328.
12. Welzel, U., Ligot, J., Lamparter, P., Vermeulen, A.C. & Mittemeijer, E.J., 2005, *J. Appl. Cryst.*, **38**, 1.
13. Gressmann, T., Leineweber, A., Mittemeijer, E.J. & Knapp, M., *in preparation*.
14. Delhez, R., de Keijser, T.H. & Mittemeijer, E.J., 1987, *Surf. Eng.*, **3**, 331.
15. TOPAS. *General Profile and Structure Analysis Software for Powder Diffraction Data* (Karlsruhe, Germany: Bruker AXS GmbH).
16. Leineweber, A. & Mittemeijer, E.J., 2004, *J. Appl. Cryst.*, **37**, 123.
17. Maldzinski, L., Przylecki, Z. & Kunze, J., 1986, *Steel Research*, **57**, 645.
18. Leineweber, A., Jacobs, H., Kockelmann, W., Hull, S. & Hinz-Hübner, D., 2004, *J. Alloys Compd.*, **384**, 1.
19. Wohlschlögel, M., Baumann, W., Welzel, U. & Mittemeijer, E.J., 2006, *Mater. Sci. Forum*, **524-525**, 19.